Recent K^0 Decay Results from Fermilab E-731

A.R. Barker
Enrico Fermi Institute
University of Chicago, Chicago, IL 60637

ABSTRACT

The status of the E-731 experiment is reviewed. In addition, preliminary results are reported from searches for three rare decays of the K^0, using data collected by the E-731 Collaboration during the 1987–88 fixed-target run at Fermilab. Branching ratio results are presented for the decays $K^0_{L,S} \to \pi^+\pi^-\gamma$, as well as for the decay $K^0_L \to \pi^\pm\pi^0 e^\mp \nu(\bar{\nu})$. An upper limit is derived for the decay $\pi^0 \to e^+e^-$, using the processes $K^0_L \to \pi^0\pi^0\pi^0$ and $K^0_L \to \pi^+\pi^-\pi^0$ to tag π^0 mesons.

INTRODUCTION

Fermilab experiment E-731 was designed to measure the CP-violating parameter ϵ'/ϵ by studying the four decays $K_{L,S} \to \pi^+\pi^-$ and $K_{L,S} \to \pi^0\pi^0$. The signature of direct CP violation, *i.e.*, a non-zero value for $\mathrm{Re}(\epsilon'/\epsilon)$, is that the ratio of the neutral to charged decay rates of the K_L would differ from the corresponding ratio for decays of the K_S. In particular, if the double-ratio R is defined by

$$R = \frac{\Gamma(K_S \to \pi^0\pi^0)/\Gamma(K_S \to \pi^+\pi^-)}{\Gamma(K_L \to \pi^0\pi^0)/\Gamma(K_L \to \pi^+\pi^-)},$$

then $\mathrm{Re}(\epsilon'/\epsilon)$ can be derived from the relation

$$\mathrm{Re}\left(\frac{\epsilon'}{\epsilon}\right) = \frac{1}{6}(R-1).$$

The challenge, then, is to measure very precisely the double-ratio R, in order to determine whether it differs slightly from unity. In order to do this, an experiment must be carefully designed to minimize systematic biases in the measurement of R. The technique chosen by the E-731 group employs two parallel K_L beams. A B_4C regerator is placed in one of the beams, providing a flux of coherently regenerated K_S mesons. Downstream of the regenerator,

most of the decays in one beam are K_S decays, and almost all of the decays in the other (vacuum) beam are K_L decays. The double ratio R is then measured by comparing the decay rates in the two beams.

This method of measuring R has the great advantage that K_L and K_S decays are detected at the same time, and by the same detector. Time-dependent changes in beam intensity or detector response thus affect K_L and K_S decays to the same final state at the same point in the decay volume in exactly the same way. In order to minimize differences that might arise as a result of differences between the two beams, the regenerator alternated from one beam to the other about once a minute.

Because the lifetimes of the K_L and K_S are so different, the distribution of values of z, the distance travelled by a kaon prior to its decay, is quite different in the vacuum beam from that observed in the regenerated beam. It is therefore necessary to simulate accurately the acceptance of the detector, which also depends on z, in order to ensure that the effects of this non-uniform acceptance on R are correctly taken into account.

In order to detect a difference between R and unity on the order of 1%, a sample of several hundred thousand examples of each of the four $K_{L,S}$ decay modes must be collected. Because the branching ratio for $K_L \to \pi^0\pi^0$ is less than 10^{-3}, and because the acceptance for this mode is roughly 20% in the z region used in the analysis, the experiment must be exposed to an integrated flux of several billion $K_{L,S}$ decays in this region alone in order to achieve the desired accuracy.

The combination of good four-body acceptance, hermeticity, and a very large integrated flux of K^0 decays which is required for the measurement of $\mathrm{Re}(\epsilon'/\epsilon)$ is also ideal for the study of a variety of rare decays. In the case of the decay $K_L \to \pi^0 e^+ e^-$, which has attracted considerable recent interest,[1] the single event sensitivity of the E-731 data set corresponded to a branching ratio of approximately 3.3×10^{-9}, almost as good as the 2.4×10^{-9} achieved[2] by a recent Brookhaven experiment (E-841) dedicated to the study of this mode. Our upper limit on $B(K_L \to \pi^0 e^+ e^-)$ was reported in Ref. 3.

In the remainder of this paper, I will describe the E-731 apparatus, then briefly review the status of the ϵ'/ϵ analysis effort. After this, I will proceed to a discussion of preliminary results on three rare decay modes. In the first of these, $K_{L,S} \to \pi^+\pi^-\gamma$, we have for the first time observed the proper-time interference between K_S and K_L in a mode other than $\pi^+\pi^-$ or $\pi^0\pi^0$. Our observation of some 800 examples of the second rare-decay mode discussed here, neutral K_{e4}, represents a dramatic increase in statistical power compared to the best published measurement of the branching ratio for that mode, which was based on a sample of 16 events. The third rare decay mode dicussed is $\pi^0 \to e^+e^-$, in which the common decays $K_L \to \pi^0\pi^0\pi^0$ and $K_L \to \pi^+\pi^-\pi^0$ provide a method of tagging π^0's. Although the branching ratio limit we obtain is a factor of two higher than the best published limit for $\pi^0 \to e^+e^-$, we are optimistic that the use of this technique with the same detector will soon result in an unambiguous observation of this interesting electromagnetic decay.

The work described here is a collaborative effort of the E-731 group, which consists at present of R.A. Briere, L.K. Gibbons, K. McFarland, G. Makoff, V. Papadimitriou, J.R. Patterson, B. Schwingenheuer, S. Somalwar, Y. Wah, B. Winstein, M. Woods, H. Yamamoto, and myself, from the University of Chicago; G. Bock, R. Coleman, J. Enagonio, B. Hsiung, E. Ramberg, K. Stanfield, R. Stefanski, R. Tschirhart, and T. Yamanaka from Fermilab; M. Karlsson from Princeton University; G. Gollin from the University of Illinois (Champaign/Urbana); E. Swallow from Elmhurst College; and P. Debu, B. Peyaud, R. Turlay, and B. Vallage of the Centre d'Etudes Nucléaires de Saclay.

THE APPARATUS

The E-731 detector is shown schematically in Fig. 1. Downstream of the regenerator is a vacuum decay volume some 30 meters long, divided into two halves by a thin scintillator hodoscope used for triggering. Photon counters around the edges of the decay volume are used to identify events in which photons escape the apparatus. Charged particles from K^0 decays are detected in a series of four drift chambers downstream of the decay volume. An analysis magnet between the second and third chambers imparts a transverse momentum kick of 200 MeV/c to a charged particle, so that the bend in the track it leaves can be used to measure its momentum. The drift chambers measure hit locations with a typical precision of 90 to 100 microns.

Beyond the last chamber, particles intercept a pair of trigger hodoscopes, then enter a lead-glass calorimeter. The calorimeter consists of 804 lead glass blocks, 5.82 cm square by 19 radiation lengths long. The calorimeter measures the energy of incident electrons with a resolution $\delta E/E$ of $1.5\% + 5\%/\sqrt{E}$ (where E is the energy in GeV). The constant term is a consequence of the absorbtion of Čerenkov light by the glass, so that the amount of light detected varies depending on the longitudinal profile of the electromagnetic shower. Because the depth of the initial conversion of photons in the glass varies, this effect is somewhat larger for photons, resulting in a photon-energy resolution of approximately $2.5\% + 5\%/\sqrt{E}$.

Electrons are identified by using the measured value of E/p, where E is the energy measured in the calorimeter, and p is the momentum derived from the drift chambers. A cut requiring that E/p be between 0.88 and 1.12, for example, accepts about 96% of all electrons while rejecting over 98% of charged pions.

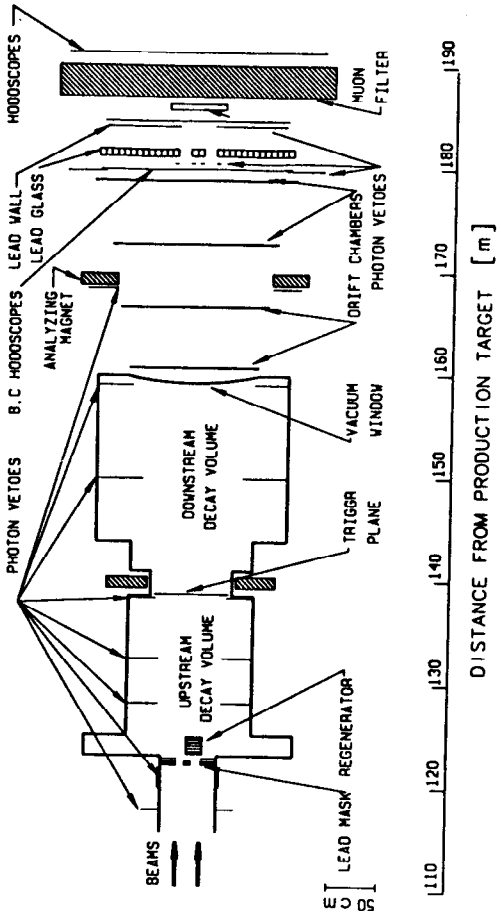

Figure 1: A schematic representation of the E-731 detector Note the differing horizontal and vertical scales.

A muon filter consisting of about three meters of steel is behind the lead glass calorimeter. Hodoscopes in front of and behind this filter allow the detection of pions and muons that penetrate the lead glass, as well as muons that penetrate both the calorimeter and the steel.

During the 1987–88 run at Fermilab, E-731 used two basic triggers. One, the neutral trigger, required the deposition of at least 27 GeV in the lead glass. Events were vetoed if a signal was observed in any of the various photon counters, or in scintillator banks behind the lead glass, or in the trigger hodoscope 14 meters downstream of the regenerator. A second-level trigger processor was activated for events satisfying these basic requirements. It identified and counted clusters of energy deposition in the calorimeter. Events with exactly four clusters (as well as a prescaled sample of six-cluster events) were selected by the processor. This trigger was designed to collect events from the decay $K_{L,S} \to \pi^0\pi^0$. Most of the events recorded, however, were from the much more common decay $K_L \to \pi^0\pi^0\pi^0$, when overlapping or missing photons resulted in there being only four clusters.

The other basic trigger was the charged trigger, designed to select events involving the decays $K_{L,S} \to \pi^+\pi^-$. This trigger required that there be hits in both the top and bottom halves of the vertically segmented hodoscope in front of the calorimeter, and that there be hits in both the left and right halves of the horizontally segmented hodoscope in the same location. In addition, hits were required in the trigger hodoscope 14 meters downstream of the regenerator. Consequently, only decays occurring upstream of that point were selected. A final requirement was that hits be detected in both the left and right halves of the second drift chamber. The principal backgrounds to $\pi^+\pi^-$ decays for this trigger were from the processes $K_L \to \pi^+\pi^-\pi^0$ and $K_L \to \pi^\pm e^\mp \nu(\bar{\nu})$.

Both the charged and neutral triggers were designed with $K_{L,S} \to \pi\pi$ decays in mind. They gave us good acceptance for most rare decay modes, including those discussed in this paper. However the triggers were strongly biased against a few modes, notably K_L Dalitz decays ($K_L \to e^+e^-\gamma$). In this mode, there are three energy clusters in the calorimeter, which would not satisfy the four- or six-cluster requirement of the neutral trigger, and the electron and positron tracks are typically very close together, so that the up-down and left-right requirements of the charged trigger quite efficiently rejected the events. Similar factors caused some modes involving π^0 Dalitz decays to fail the trigger requirements.

In all, some eight million examples of the decay $K_L \to \pi^+\pi^-\pi^0$, 20 million of the decay $K_L \to \pi^0\pi^0\pi^0$, and 120 million K_{e3} decays, were written to tape during the run. The enormous number of events observed in each of these modes has allowed us to perform extremely detailed studies of acceptance, beam shape, calorimeter response, and drift chamber alignment, all of which have been crucial to our understanding of the $\pi\pi$ data. The Monte Carlo simulation of the

detector relies on only a small number of tunable parameters, including the momentum spectra of K^0 and $\overline{K}^0$ mesons produced at the target, the relative intensity of the upper and lower beams, and the shapes and positions of the beams. Nevertheless, it is able to reproduce a wide variety of distributions for the various high-statistics modes we have studied with impressive accuracy. For example, Fig. 2 shows the observed distribution of z, the distance between the target and the decay vertex in K_{e3} events. The distribution predicted by the Monte Carlo distribution is also shown; the ratio of data to Monte Carlo is shown in the second part of the figure.

We have also studied the effects of accidental backgrounds on our acceptance by overlaying real events from accidental triggers on top of simulated events representing K_L or K_S decays to various modes, including various rare decays as well as $\pi\pi$ final states. In the case of the $\pi\pi$ decays, we find that accidental backgrounds affect the K_L and K_S rates by exactly the same amount, to within a statistical error of less than 0.1%. To extract rare decay branching ratios, we need to know the relative effects of accidentals on the acceptance for the mode being studied and on that for the mode being used for normalization. This we have also done by using accidental overlays in the Monte Carlo.

STATUS OF ϵ'/ϵ ANALYSIS

During most of the 1987–88 run, charged-trigger and neutral-trigger data were taken separately, either one trigger or the other being disabled. Towards the end of the run, however, both triggers were enabled simultaneously. About 20% of out total exposure was obtained while running in this way, and it is this part of the data that was analysed first. The result of that analysis,

$$\mathrm{Re}\left(\frac{\epsilon'}{\epsilon}\right) = (-4 \pm 14 \pm 6) \times 10^{-4},$$

was reported in Ref. 4. This value is consistent with superweak models,[5] which predict that ϵ' vanishes, as well as with recent theoretical predictions[6] within the Standard Model, which include the effects of so-called "Z-penguin" diagrams and a large top-quark mass. It does not, however, confirm the NA31 report[7] of a value for $\mathrm{Re}(\epsilon'/\epsilon)$ significantly different from zero.

The uncertainty in the partial E-731 result is dominated by the statistical error, which should be reduced to about 5×10^{-4} once the analysis of the full data set is complete. Figure 3 shows the mass spectra for the four $K_{L,S} \to \pi\pi$ modes; all the 1987–88 data are included. Further work on understanding possible systematic errors is in progress; at present we believe that the final systematic error will be no greater than 4×10^{-4}. In addition to the ϵ'/ϵ result,

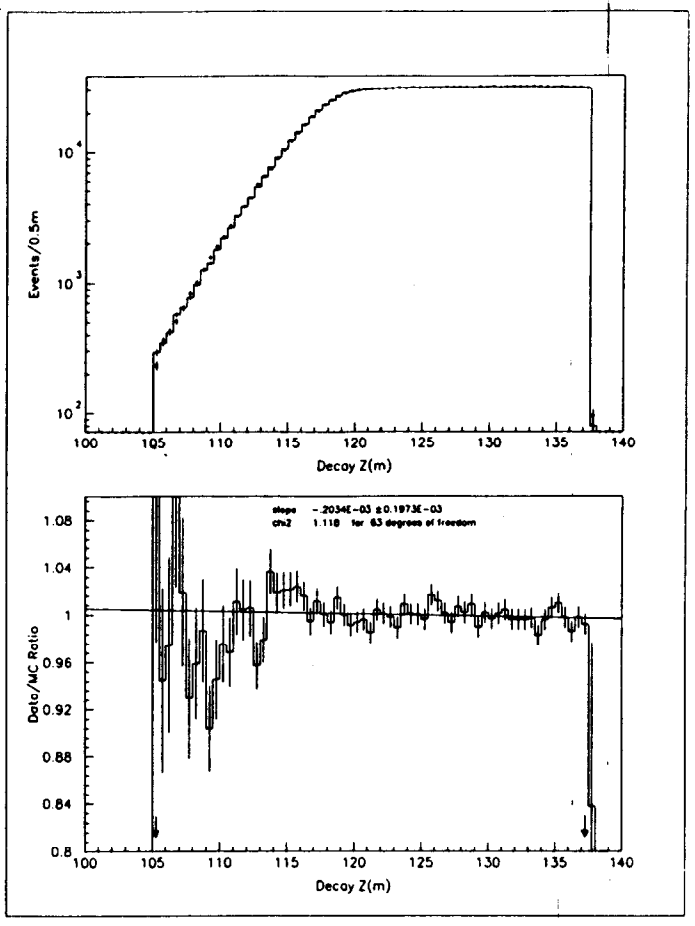

Figure 2: A typical comparison between data and Monte Carlo for one of the high-statistics modes used for calibration. The top part of the figure shows the distribution of decay vertex locations for K_{e3} events in the data (the histogram) and as predicted by the Monte Carlo (the solid dots with errors). The bottom part shows the ratio Data/Monte Carlo, which should be consistent with one for all values of z. The best linear fit is shown; the slope is about one standard away from zero.

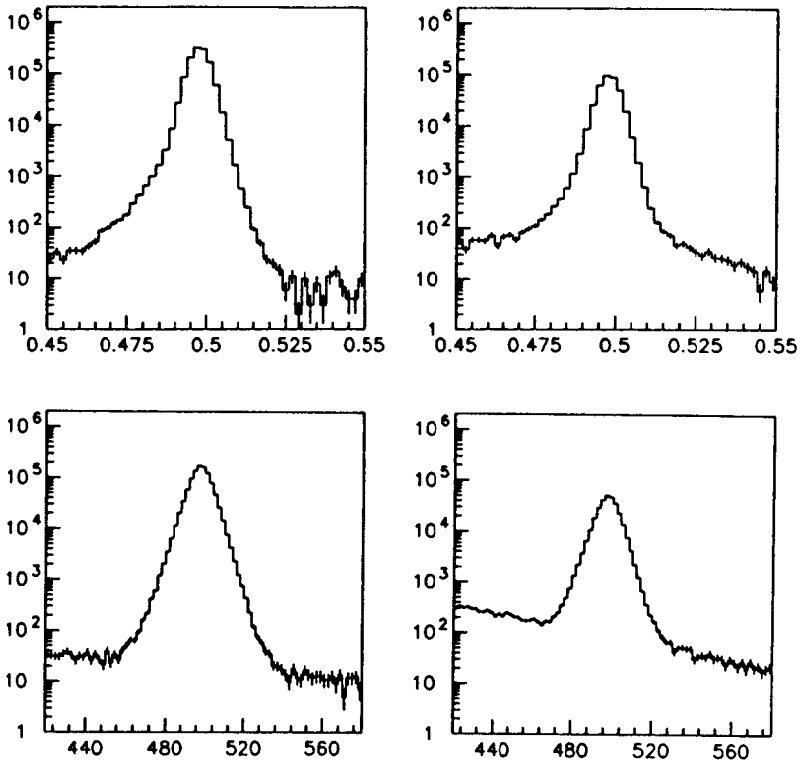

Figure 3: The invariant mass spectra for the four $\pi\pi$ decay modes of the K^0. All E-731 data are included. Upper left: $K_S \to \pi^+\pi^-$; Upper right, $K_L \to \pi^+\pi^-$; Lower left: $K_S \to \pi^0\pi^0$; Lower right: $K_L \to \pi^0\pi^0$.

we have also published[8] a result for the difference in the phases of the CP-violating amplitudes η_{00} and η_{+-}:

$$\phi_{00} - \phi_{+-} = -0.3 \pm 2.4 \pm 1.2^\circ.$$

A difference between ϕ_{00} and ϕ_{+-} of more than about 0.15° would be a sign of CPT violation.[9] Our group, with the addition of new collaborators from Rutgers, plans to perform a more precise measurement of the phase difference during experiment E-773, which will take place during the 1991 fixed-target run at Fermilab.

STUDY OF $K_{L,S} \to \pi^+\pi^-\gamma$

Careful inspection of the $\pi^+\pi^-$ invariant mass plots in Fig. 3. reveals the presence of a non-Gaussian low-mass tail, which is due to radiative decays, $K_{L,S} \to \pi^+\pi^-\gamma$. These decays are interesting in their own right; we have analysed a sample of $\pi^+\pi^-\gamma$ decays in which the photon was sufficiently energetic and well-separated from the pions to be unambiguously identified. In this section, I describe some preliminary results from an analysis of these events.

The reactions $K_S \to \pi^+\pi^-\gamma$ and $K_L \to \pi^+\pi^-\gamma$ are in fact quite different. The former decay is dominated by the "internal bremsstrahlung" process, in which a photon is radiated by one of the charged pions produced at the $K_S\,\pi^+\pi^-$ vertex. The rate for this decay, compared to that for $K_S \to \pi^+\pi^-$, has been calculated[10] from QED:

$$\frac{d\Gamma}{dk\,d\cos\theta} = \frac{2\alpha}{\pi}\Gamma(K_S \to \pi^+\pi^-)\frac{1}{E^*_\gamma}\left(1 - \frac{2E^*_\gamma}{M_K}\right)\frac{\beta^3\sin^2\theta}{\beta_0(1-\beta^2\cos^2\theta)^2},$$

where

$$\beta = \left(1 - \frac{4m_\pi^2}{M_K^2 - 2M_K E^*_\gamma}\right)^{1/2}$$

and $\beta_0 = \beta(E^*_\gamma = 0)$. In these formulae, E^*_γ is the energy of the radiated photon in the kaon rest frame, M_K is the kaon mass, m_π the charged pion mass, and θ is the angle between the photon and the π^+ three-momenta in the kaon rest frame. The predicted ratio between the radiative decay (with $E^*_\gamma > 50$ MeV) and the non-radiative decay is 2.55×10^{-3}.

In the K_L decay to $\pi^+\pi^-\gamma$, the contribution from inner bremsstrahlung should occur at the same rate relative to the $\pi^+\pi^-$ mode, but both modes are CP-violating, and are suppressed by a factor of $|\epsilon|^2$. However, the decay

$K_L \to \pi^+\pi^-\gamma$ can also conserve CP if it occurs by means of an "$M1$ direct emission" transition, for which the effective Lagrangian is

$$\mathcal{L}_{eff} = g\epsilon_{\alpha\beta\gamma\delta}p_+^\alpha p_-^\beta k^\gamma e^\delta,$$

where e is the photon polarization vector, and p_+, p_-, and k are the four-momenta of the π^+, π^-, and photon, respectively. CP-violating "$E1$" direct emission is also possible, as are higher multipole radiative transitions. The direct emission contribution to the $K_L \to \pi^+\pi^-\gamma$ decay rate can be extracted relatively easily because the photon energy spectrum resulting from direct emission, which rises as E_γ^{*3} for small values of E_γ^*, is dramatically different from the $1/E_\gamma^*$ behaviour characteristic of inner bremsstrahlung.

Examples of the decays $K_{L,S} \to \pi^+\pi^-\gamma$ were selected from the charged-trigger data by requiring that events satisfy the following criteria:

- They had to contain two good tracks, each with a measured momentum greater than 7 GeV/c, and with opposite charges.
- Each track had to be matched to an energy cluster of at least 500 MeV in the lead glass calorimeter, and the value of E/p had to be less than 0.8. This cut removed backgrounds from K_{e3} decays with accidental photons.
- There had to be exactly one additional energy cluster in the lead glass, not matched to either track, and the energy of this cluster had to exceed 1.5 GeV. The relatively high energy requirement helps to reduce accidental backgrounds, since accidental photons tend to have smaller energies than those from K^0 decays.
- The decay vertex, determined from the extrapolated point of closest approach of the two tracks, had to be no more than 137.5 meters downstream of the target, which is just upstream of the trigger hodoscope.
- The total energy of the two pions and the photon had to be less than 160 GeV. This cut removed background from $\Lambda \to p\pi^-$ decays with accidental photons, since Λ's with momenta below this cut virtually never survive long enough to reach the decay region.
- The vector sum of the components of the pion and photon momenta transverse to the K^0 line-of-flight had to have a squared magnitude of less than 250 MeV$^2/c^2$. This reduced non-exclusive backgrounds, like $\pi^+\pi^-\pi^0$ with a missing photon, and selected only coherently regenerated K_S mesons.

After these cuts, the remaining events already are a reasonably pure sample of $\pi^+\pi^-\gamma$ decays. The principal residual background is from $K_L \to \pi^+\pi^-\pi^0$ decays in which one of the two photons from the π^0 decay was not detected. To reduce this background even further, we use a kinematic quantity called $(P_{\pi^0}^L)^2$, defined by

$$(P_{\pi^0}^L)^2 \equiv \frac{(M_{K^0}^2 - M_{\pi^0}^2 - M_{\pi^+\pi^-}^2)^2 - 4M_{\pi^0}^2 M_{\pi^+\pi^-}^2 - 4M_{K^0}^2(P_{\pi^+\pi^-}^T)^2}{4(M_{\pi^+\pi^-}^2 + (P_{\pi^+\pi^-}^T)^2)}.$$

Here $P_{\pi^+\pi^-}^T$ is the sum of the transverse momenta of the charged pions, and $M_{\pi^+\pi^-}$ is their invariant mass. Aside from resolution effects, this quantity must be positive if the event was a $\pi^+\pi^-\pi^0$ decay with a missing photon, since it would then equal the square of the π^0 longitudinal momentum. Here, "transverse" and "longitudinal" are defined relative to the K^0 line of flight. The solid histogram in Fig. 4 shows the distribution of this quantity for the data satisfying the cuts listed above. The large peak at positive values is due to $\pi^+\pi^-\pi^0$ decays. The dashed histogram shows the distribution for events in which the $\pi^+\pi^-\gamma$ invariant mass is within 14 MeV/c^2 of the K^0 mass. It is clear that after this cut any contribution from $\pi^+\pi^-\pi^0$ decays is already very small. Nevertheless, we further reduce background from that source by requiring

$$(P_{\pi^0}^L)^2 < -0.05 \ \text{GeV}/c^2.$$

Figure 5 shows the $\pi^+\pi^-\gamma$ invariant mass distribution in the K^0 mass region after all cuts. A clear peak containing over eight thousand events is seen, with negligible background. Of these, slightly more than half are decays in the regenerator beam. For subsequent analysis, we selected events whose invariant masses were within 14 MeV/c^2 of the nominal K^0 mass. Figure 6 shows the K^0 center-of-mass energy spectrum of the photons in these decays in both the regenerator and the vacuum beam. In the regenerator beam, where the vast majority of decays are $K_S \to \pi^+\pi^-\gamma$, the steeply falling energy spectrum characteristic of inner bremsstrahlung is observed. In the vacuum beam, the spectrum below 40 MeV is similar to the K_S spectrum, indicating the presence of the CP-violating inner bremsstrahlung contribution to $K_L \to \pi^+\pi^-\gamma$. However, above 40 MeV the spectrum is radically different, showing the prominent peak at higher energies which is the signature of the direct emission K_L decay.

In the case of the K_S, we estimate that 4563 of the 4745 $\pi^+\pi^-\gamma$ events in the regenerator beam with with $E_\gamma^* > 20$ MeV are due to K_S decays. In 1590 of these events, the photon energy was greater than 50 MeV in the K_S rest frame. The total number of $K_S \to \pi^+\pi^-$ decays occuring in the fiducial volume during this run was estimated to be about 2.75 million. Given our average experimental acceptance of about 25% (calculated from a Monte Carlo simulation of the detector and analysis procedure), this yields a branching ratio measurement:

$$\frac{B(K_S \to \pi^+\pi^-\gamma; E_\gamma^* > 50 \text{ MeV})}{B(K_S \to \pi^+\pi^-)} = (2.38 \pm 0.06 \pm 0.04) \times 10^{-3},$$

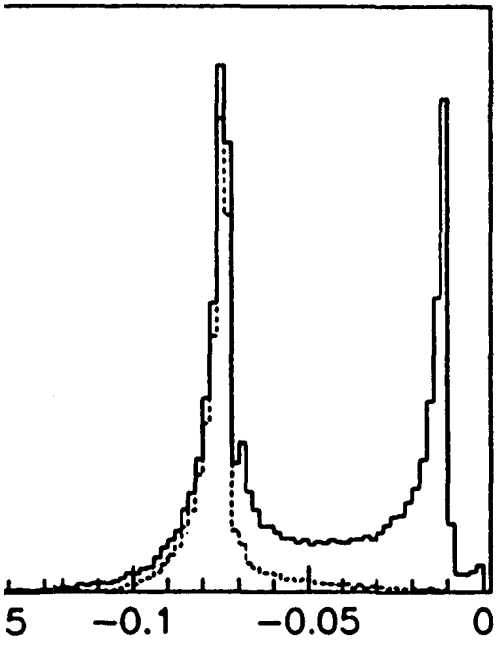

'he diribution of $(P^L_{\pi^0})^2$ values for events
atisfyg the $\pi^+\pi^-\gamma$ selection criteria. The solid
istogm includes all events; the dashed histogram,
nly tlse with a $\pi^+\pi^-\gamma$ invariant mass within
4 Me/c^2 of the nominal K^0 mass.

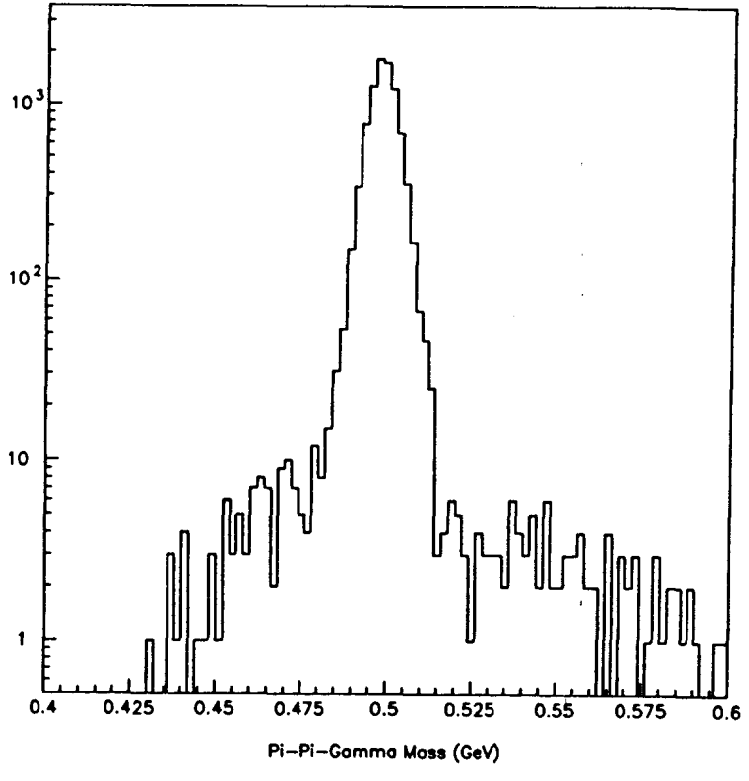

Figure 5: The spectrum of $\pi^+\pi^-\gamma$ invariant masses for events satisfying the $\pi^+\pi^-\gamma$ selection criteria, including the cut on $(P^L_{\pi^0})^2$ described in the text. Events within 14 MeV/c^2 of the K^0 mass were selected for further analysis.

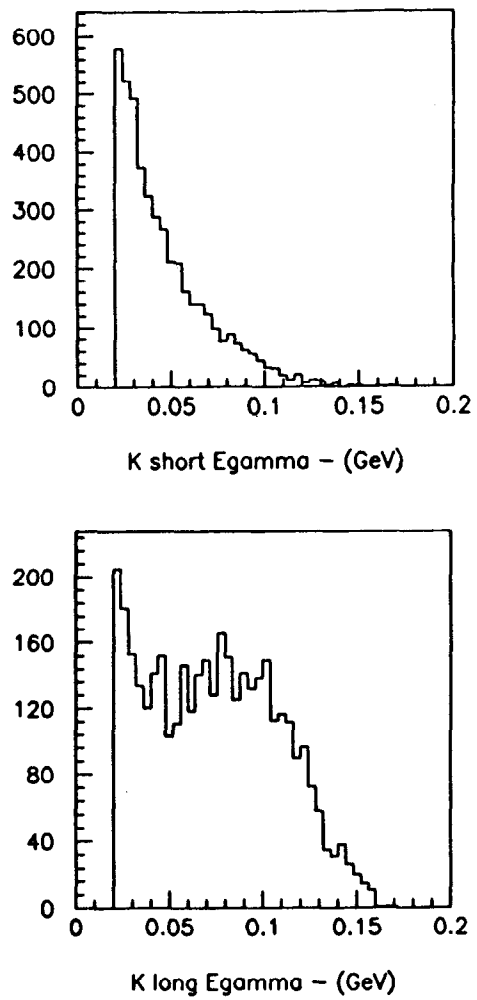

Figure 6: The spectra of center-of-mass photon energies for photons produced in the radiative decays $K_{S,L} \to \pi^+\pi^-\gamma$. The top part of the figure shows the spectrum for K_S decays, which are dominated by inner bremsstrahlung. The bottom part shows the spectrum for K_L decays, which also include a relatively large direct emission component.

which is in reasonable agreement with the theoretical prediction of 2.55×10^{-3}, and with the value of $(2.68 \pm 0.15) \times 10^{-3}$ for this ratio reported in Ref. 10. We are able to identify $\pi^+\pi^-\gamma$ decays of the K_S with good efficiency even when the radiated photon is as soft as 20 MeV in the K_S rest frame, so we also report a second branching ratio result:

$$\frac{B(K_S \to \pi^+\pi^-\gamma; E^*_\gamma > 20 \text{ MeV})}{B(K_S \to \pi^+\pi^-)} = (6.36 \pm 0.09 \pm 0.05) \times 10^{-3}.$$

This preliminary result is about 10% below the theoretical prediction of 7.00×10^{-3}.

For the K_L decay, we want to measure separately the inner bremsstrahlung and direct emission contributions to the branching fraction. In order to do this, we have fit the $K_L \to \pi^+\pi^-\gamma$ photon energy spectrum to a linear combination of the K_S spectrum (which is assumed to be the same as the K_L inner bremsstrahlung spectrum) and a Monte Carlo prediction for the photon energy spectrum resulting from the direct emission K_L decay. The result of this fit is that the total number of inner bremsstrahlung events with $E^*_\gamma > 20$MeV in the $K_L \to \pi^+\pi^-\gamma$ data is 1453 ± 38. The average acceptance for these inner bremsstrahlung events is calculated from Monte Carlo simulations to be 12.3%. During the same run, the total number of $K_L \to \pi^+\pi^-$ decays was estimated to be 1.49 million. This yields a branching ratio of

$$\frac{B(K_L \to \pi^+\pi^-\gamma; \text{ Inner Bremss., } E^*_\gamma > 20 \text{ MeV})}{B(K_L \to \pi^+\pi^-)} = (6.49 \pm 0.17 \pm 0.20) \times 10^{-3},$$

very close to the ratio observed in K_S decays. This represents a significant improvement in statistical precision compared to the previous measurement of $(7.5 \pm 0.8) \times 10^{-3}$ reported by Carroll *et al.* in Ref. 11.

After subtracting the inner bremsstrahlung component from the $K_L \to \pi^+\pi^-\gamma$ photon energy spectrum, we are left with the spectrum shown in Fig. 7. There, the observed spectrum is compared to the spectra predicted by two different models for direct emission.[13] The second model, which predicts a shape more similar to that observed in the data, is based on a Vector-Meson Dominance model; the first model is the prediction of a Born approximation without VMD form factors.

The best fit corresponded to a total of 2363 direct emission $K_L \to \pi^+\pi^-\gamma$ decays, which implies

$$B(K_L \to \pi^+\pi^-\gamma; \text{ Direct Emission}) = (2.95 \pm 0.06 \pm 0.09) \times 10^{-5},$$

given the average acceptance of 10.9% predicted by the Monte Carlo simulation. The systematic error includes a 2% contribution from the uncertainty in the

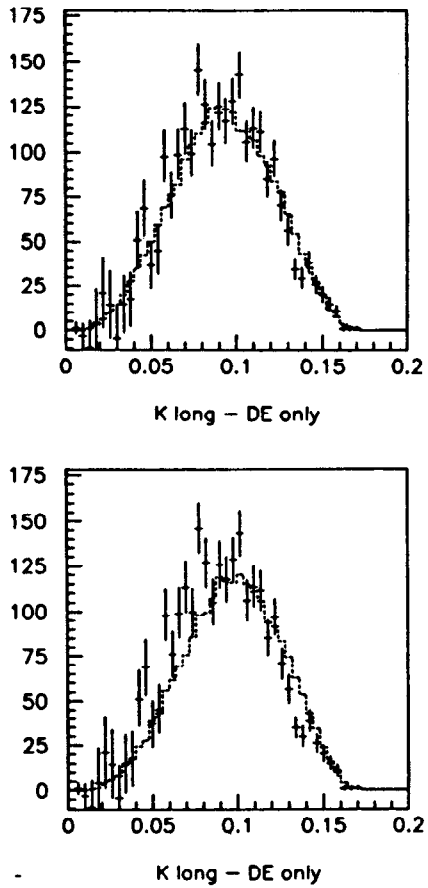

Figure 7: The photon energy spectrum for the direct emission component of $K_L \to \pi^+\pi^-\gamma$ decays, compared to Monte Carlo predictions using two different models. The data are represented by the points with error bars; the Monte Carlo predictions are the dashed histograms. The top part of the figure shows the prediction of a Born approximation; the bottom part shows instead a prediction including the effects of Vector Meson Dominance form factors, as suggested in Ref. 13.

branching ratio for $K_L \to \pi^+\pi^-$.[12] The best previous result, also from Carroll *et al.*,[11] was $(2.89 \pm 0.28) \times 10^{-5}$.

Finally, we have plotted the proper time distribution of $\pi^+\pi^-\gamma$ decays in the regenerator beam. Figure 8 shows the observed distribution, together with the distributions expected with and without K_L–K_S interference. It is clear that the observed distribution cannot be explained without K_L–K_S interference. We have fit the observed distribution for the value of $\eta_{+-\gamma}$, and our preliminary result is

$$|\eta_{+-\gamma}| = (2.0 \pm 0.5) \times 10^{-3}.$$

In the absence of direct CP-violation effects in the $\pi^+\pi^-\gamma$ decay, and of contributions from direct emission, this parameter would be equal to $|\epsilon|$. We expect the error on this measurement to decrease, and we will also extract the phase of $\eta_{+-\gamma}$ from the fit. This represents the first observation of the K_L–K_S interference in any decay mode other than $\pi^+\pi^-$ and $\pi^0\pi^0$.

STUDY OF $K_L \to \pi^\pm\pi^0 e^\mp\nu(\bar{\nu})$

Another rare decay mode we have studied is $K_L \to \pi^\pm\pi^0 e^\mp\nu(\bar{\nu})$, called K_{e4}. This mode has been extensively studied in $K^\pm$ decays[14], but the largest sample of neutral K_{e4} decays previously obtained consisted of only 16 events[15]. Theoretical interest in this mode has focussed on the "singularly rich kinematic structure"[16] of the four-body final state, which is described by no fewer than nine form factors. The five kinematic variables describing the final state can be taken to be s_π, the squared $\pi^\pm\pi^0$ invariant mass, s_l, the squared $e^\mp\nu$ invariant mass, θ_l, the angle between the electron momentum and the $\pi^\pm\pi^0$ momentum in the $e^\mp\nu$ rest frame, θ_π, the angle between the $\pi^\pm$ momentum and the $e^\mp\nu$ momentum in the $\pi^\pm\pi^0$ center of mass, and ϕ, the angle between the normal to the plane containing the lepton momenta and the normal to the plane containing the pion momenta. The short-distance electroweak part of the matrix element can be evaluated, after which the cross section can be expressed (see, for example, Ref. 16) as a sum of nine contributions. Each has a different dependence on the variables θ_l and ϕ:

$$\begin{aligned}\frac{d^6\Gamma(K_L \to \pi^\pm\pi^0 e^\mp\nu(\bar{\nu}))}{ds_\pi\, ds_l\, d\cos\theta_\pi\, d\cos\theta_l\, d\phi} &= I_1 + I_2\cos 2\theta_l + I_3 \sin^2\theta_l \cos 2\phi \\ &+ I_4 \sin 2\theta_l \cos\phi + I_5 \sin\theta_l \cos\phi + I_6 \cos\theta_l \\ &+ I_7 \sin\theta_l \sin\phi + I_8 \sin 2\theta_l \sin\phi + I_9 \sin^2\theta_l \sin 2\phi.\end{aligned}$$

Each of the form factors I_j is a function of the other three kinematic variables, s_l, s_π, and θ_π. Considerable theoretical interest has focussed on I_9, which is

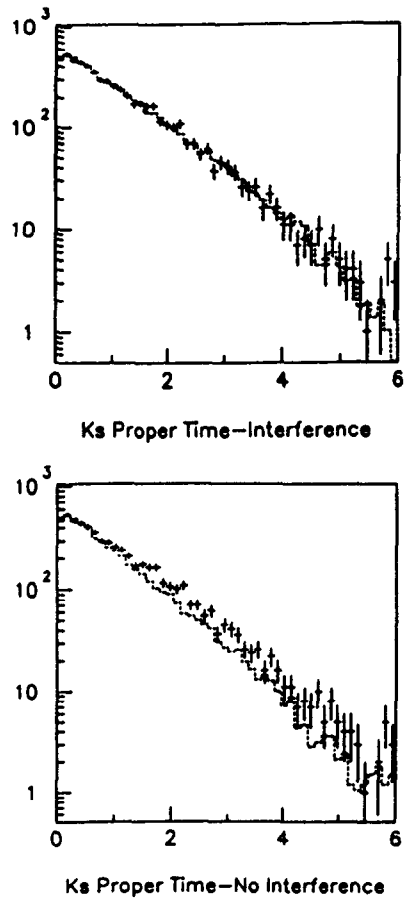

Figure 8: The proper-time interference in $K^0 \to \pi^+\pi^-\gamma$ decays. In both parts of the figure, the points with error bars show the observed proper time distribution of decays in the regenerator beam. The dashed histogram in the top part of the figure is the prediction of a Monte Carlo with no K_L–K_S interference. The data agree much better with the dashed histogram in the bottom part of the figure, which includes the amount of interference expected if $\eta_{+-\gamma} = \eta_{+-}$. Units on the abscissae are K_S lifetimes.

expected to be very small in the absence of non-Standard-Model CP violation. In Ref. 17, Castoldi, Frere, and Kane remark that measurements of I_9 are complimentary to those of ϵ'/ϵ and the neutron electric dipole moment, since only non-Standard-Model CP-violating effective Lagrangians with vector or axial vector interactions will contribute to I_9, while scalar or pseudoscalar interactions will contribute to the other measurements.

In addition, measurements of the I_j in charged kaon decays have been used to evaluate $\pi\pi$ phase shifts[18,14] and to test the $\Delta I = 1/2$ Rule. Because the $\pi\pi$ system in neutral K_{e4} decays is mostly in an $I = 0, l = 0$ state, in contrast to the charged case, in which the $\pi\pi$ state is predominantly $I = 1, l = 1$, the I_j measured in K_L decays are expected to be quite different from those already measured in $K^\pm$ decays. Thus the study of neutral K_{e4} decays should, with adequate statistics, provide information which is complimentary to what has already been learned from charged K_{e4} decays.

The K_{e4} event selection procedure included the following requirements:

- The event had to have two tracks, each with a measured momentum greater than 2.5 GeV/c (which is approximately the smallest detectable momentum, anyway), and with opposite charges.
- Both tracks had to be matched to energy clusters of at least 500 MeV. One track then had to have an E/p value less than 0.8; this track was the charged pion candidate. The other track had to have $0.9 < E/p < 1.1$; this was the electron candidate. The cluster matched to the electron-candidate track had to satisfy cuts on shower-shape parameters designed to reject hadronic showers.
- In addition to the two matched clusters, there had to be two additional, unmatched clusters, each with an energy greater than 2.1 GeV. As in the case of the $\pi^+\pi^-\gamma$ analysis, this minimum energy requirement helped to reduce accidental backgrounds. These two clusters were the photon candidates.
- Finally, the invariant mass of the two photon candidates had to be within 10 MeV/c^2 of the nominal π^0 mass. Events in sidebands outside this region were used later in the analysis to estimate the amount of residual background under the π^0 mass peak.

After these cuts, there were three main sources of background. First, $K_L \to \pi^+\pi^-\pi^0$, with one of the charged pions misidentified as an electron. The probability of such a misidentification can be estimated from $K_L \to \pi^+\pi^-\pi^0$ events by looking at the distribution of the larger of the two E/p values for events in which the shower with the larger E/p value passes the shower-shape cut mentioned above; it has been found to be about 3%. Since the $\pi^+\pi^-\pi^0$ branching fraction is 12.7%, this still contributes a background at a level of

approximately 4×10^{-3}, which is much larger than the expected level for K_{e4} decays. To further reduce this background, we attempt to reconstruct the event as a $K_L \to \pi^+\pi^-\pi^0$ decay, then reject events which have $\pi^+\pi^-\pi^0$ invariant masses and total transverse momenta within the region which, according to a Monte Carlo simulation, should be populated by $\pi^+\pi^-\pi^0$ decays. This procedure allows us to reduce the ultimate level of $\pi^+\pi^-\pi^0$ background to a level of about 10^{-6} per K_L decay (*i.e.*, the same number of signal events would imply a K_{e4} branching fraction of 10^{-6}). The remaining background from this source is subtracted by a procedure which is described in detail below.

The second source of background is radiative K_{e3} decays in coincidence with an accidental photon, such that the two photons combine to form a fake π^0. We reduce this background by requiring that $p_e \cdot p_\gamma$ be greater than 50 MeV$^2/c^2$. Since the matrix element for radiative K_{e3} decays is inversely proportional to this quantity, most such decays are rejected by this cut.

The final background source is K_{e3} decays with two accidental photons which combine to form a fake π^0. This background source, together with radiative K_{e3} background events which survive the $p_e \cdot p_\gamma$ cut, is supressed by a requirement that $M_{\pi\pi e}$, the invariant mass of the observed particles, be not more than 5 MeV/c^2 greater than the nominal K^0 mass. All real K_{e4} events should satisfy this cut, but some events with accidental photons do not. In addition, we require that

$$\frac{(M_K^2 - M_{\pi\pi e}^2)^2}{4M_K^2} > -1500 \text{ MeV}^2/c^4.$$

For a real K_{e4} decay, this quantity is the square of the neutrino's longitudinal momentum (i.e., the component parallel to the K^0 line-of-flight) and must therefore be non-negative. The slightly negative cut allows for the effects of finite energy and momentum resolution.

The $\gamma\gamma$ invariant mass spectrum for all events surviving these cuts is shown in Fig. 9. There is a clear peak at the π^0 mass containing roughly 800 events, as well as a slowly falling background. The shape of the peak is in good agreement with the prediction of the Monte Carlo, also shown in Fig. 9. The slowly falling background is due to the presence of the K_{e3} and radiative K_{e3} backgrounds, in which the $\gamma\gamma$ mass spectrum should not show at peak at the π^0 mass. We take advantage of this fact to estimate the background under the peak due to these sources from the sidebands in $M_{\gamma\gamma}$. This yields an estimate of 121 ± 30 background events from K_{e3} and radiative K_{e3} decays with accidental photons. The uncertainty is systematic, and reflects our uncertainty as to the exact shape of the $M_{\gamma\gamma}$ mass spectrum for these accidental backgrounds.

The other background source, $\pi^+\pi^-\pi^0$ events which survive all the cuts described above, does contain a π^0, and therefore contributes to the peak in

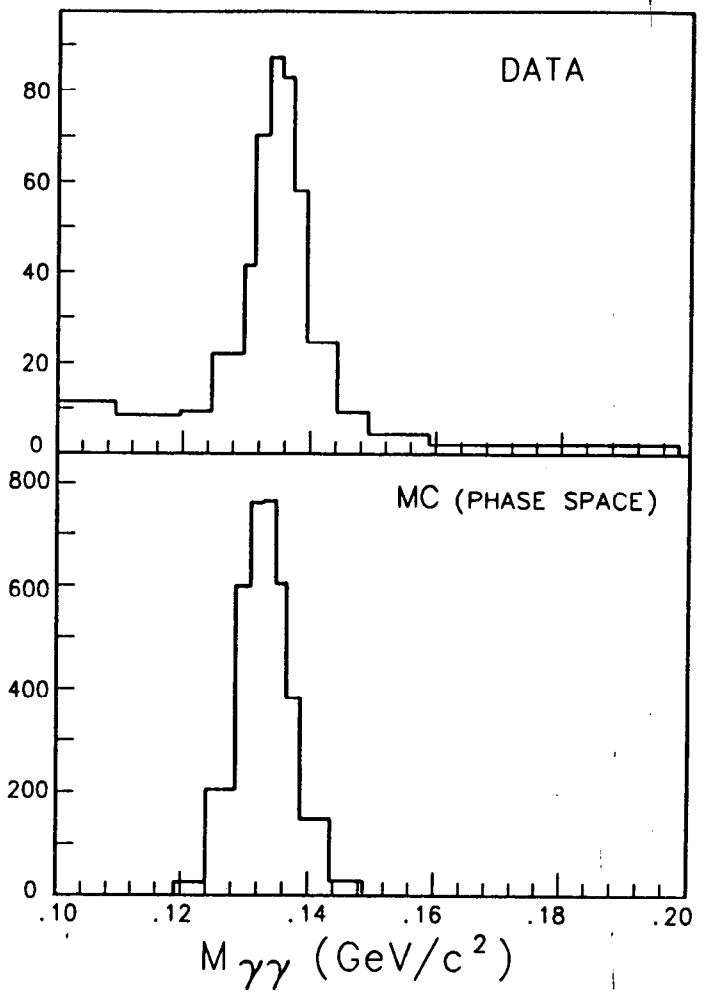

Figure 9: The $\gamma\gamma$ invariant mass distribution for events satisfying the K_{e4} selection criteria. The top part of the figure shows the observed distribution; the bottom part, the prediction of a phase space Monte Carlo simulation.

the $M_{\gamma\gamma}$ spectrum, and not to the sidebands. Figure 10 shows the distribution of the maximum E/p values for the remaining events, after the subtraction based on the $\gamma\gamma$ mass spectrum. The peak centered at an E/p value of unity demonstrates that the data consist primarily of K_{e4} events, rather than $\pi^+\pi^-\pi^0$ events which somehow survive to this stage of the analysis.

The amount of residual $\pi^+\pi^-\pi^0$ background is estimated from the data by using instead an E/p sideband in which the larger E/p value for two tracks was between 0.7 and 0.9. Very few electrons have measured E/p values below 0.9, so we assume that this sideband is populated exclusively by $K_L \to \pi^+\pi^-\pi^0$ events. Using a sample of good $\pi^+\pi^-\pi^0$ events in the data, we found that the ratio of the number of events with the larger E/p value between 0.9 and 1.1 to the number in which this value was between 0.7 and 0.9 was 0.42. Therefore, we estimated the $\pi^+\pi^-\pi^0$ background remaining after all cuts by scaling the number of sideband events in each $M_{\gamma\gamma}$ bin by 0.42, then subtracting this number from the ovserved $M_{\gamma\gamma}$ spectrum. This method leads to a total subtraction of 28 events. Pending further study of this subtraction procedure, we conservatively estimate the uncertainty in this background at ± 10 events.

The total number of events in the $M_{\gamma\gamma}$ spectrum with $|M_{\gamma\gamma} - M_{\pi^0}| < 10$ MeV/c^2 is 929. After subtracting the background by the methods just described, we find that the number of K_{e4} events in this region is 780 ± 40. From the Monte Carlo simulation, we find that our average acceptance for this mode was about 1.2%, assuming that the decays are distributed simply according to phase space. We have tried one other matrix element, and found essentially the same acceptance, but we cannot exclude the possibility of a significant correlation between the K_{e4} form factors and the acceptance. Nevertheless, if we combine the phase-space acceptance with our total exposure of 1.07×10^9 K_L decays while running with the charged trigger enabled, we find a branching fraction for the K_{e4} mode of $(5.8 \pm 0.2) \times 10^{-5}$, where the error is statistical only. Our estimate for the systematic error due to background subtraction is ± 40 events, as has been noted above. The following table lists our preliminary estimates for this and other sources of systematic error:

• Background Subtraction Technique	5%
• Effects of $\pi^\pm$ Showers	2%
• Accidental Effects	3%
• Normalization	2%
• Acceptance	2%.

Combining these estimates in quadrature, we get a total systematic error of 6.8%, which yields our preliminary result:

$$B(K_L \to \pi^\pm\pi^0 e^\mp \nu(\bar{\nu})) = (5.8 \pm 0.2 \pm 0.4) \times 10^{-5}.$$

We hope that further study will enable us to reduce the total systematic error to

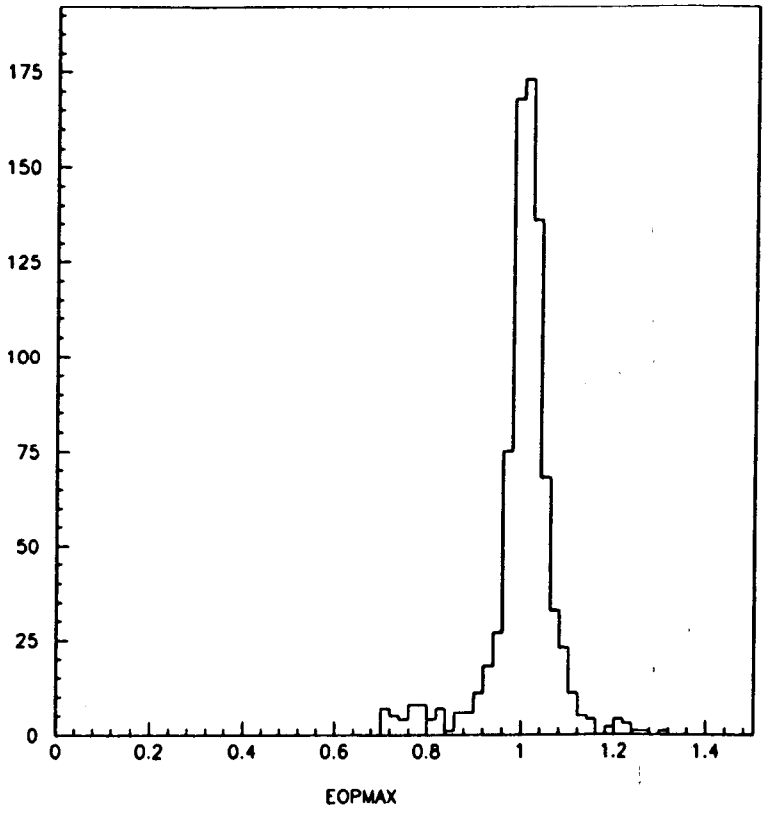

Figure 10: The distribution of E/p values for events satisfying the K_{e4} selection criteria, and having $\gamma\gamma$ invariant masses within 10 MeV/c^2 of the nominal π^0 mass. Misidentified $\pi^+\pi^-\pi^0$ events would contribute a relatively flat background beneath the peak produced by real K_{e4} events.

perhaps half the level we quote here. I emphasize once more that this result is valid only for a phase-space matrix element, and that the systematic error does *not* reflect variations in the result which may occur as a result of changes in the form of the matrix element. We have begun to investigate angular correlations in the K_{e4} sample, and we intend ultimately to fit the data for the various form factors, and to study the dependence of the acceptance on the matrix element.

SEARCH FOR $\pi^0 \to e^+e^-$

The order α^4 eletromagnetic decay $\pi^0 \to e^+e^-$ has been the subject of considerable interest, since the smallness of the Standard Model branching fraction may permit new interactions to reveal themselves.[19] The best current upper limit on the branching fraction for this mode comes from the recent SINDRUM experiment[20], from which a 90% confidence level upper limit of 1.3×10^{-7} was reported. The amplitude for this process has two parts, the real, absorbtive part, which can be confidently predicted from QED, and the imaginary, dispersive part, which depends on the electromagnetic form factor of the π^0. The branching fraction cannot be less than the value calculated by assuming that the dispersive part of the amplitude vanishes; this level, the so-called unitarity limit for $\pi^0 \to e^+e^-$, would correspond to a branching fraction of 4.8×10^{-8}. Recent calculations of the dispersive amplitude[21] lead to a more realistic prediction for the branching fraction in the range $6\text{–}7\times10^{-8}$.

The main experimental challenge in the measurement of this mode is how to "tag" the decaying π^0; that is, how to measure accurately its momentum in order to see that the e^+e^- pair observed in the detector really resulted from the decay of a π^0 to those two particles and no others. The SINDRUM experiment did this by detecting the neutron produced in the reaction $\pi^-\mathrm{p} \to \mathrm{n}\pi^0(\pi^0 \to e^+e^-)$, where the negative pion was incident on a stationary proton. They nevertheless had to deal with a sizable background from the process $\pi^-\mathrm{p} \to \mathrm{n}e^+e^-$, where the e^+e^- pair accidentally combined to give a π^0 mass. They did this by fitting the observed e^+e^- mass spectrum and looking for a peak at the π^0 mass.

In the 1978 experiment of Fischer *et al.*[22], neutral pions were produced in the decay $K^\pm \to \pi^\pm\pi^0$. The π^0 could therefore easily be tagged by measuring the momentum of the decaying kaon and the charged pion in the final state. In constrast to the π^-p interaction technique, the rate for $K^\pm \to \pi^\pm e^+e^-$ is extremely small, and contributes a background far below the unitarity limit to $\pi^0 \to e^+e^-$. The problem with this method however, is that the available flux of kaon decays was simply too small to be sensitive to $\pi^0 \to e^+e^-$ decays at the level predicted by QED. The 1978 CERN experiment did observe six events, with a background estimated at about one event, on the basis of which they reported a branching ratio of $(2.2 \pm 0.7) \times 10^{-7}$. A value of 2.2×10^{-7} is much larger than the predictions and would be difficult to explain theoretically; however, the statistical error on the result is large.

We have used the large number of K_L decays to $\pi^0\pi^0\pi^0$ and $\pi^+\pi^-\pi^0$ in the E-731 data to tag neutral pions, and thereby search for the $\pi^0 \to e^+e^-$ mode. The former mode is particularly attractive, since every K_L decay produces three π^0's, any one of which can then decay to e^+e^-. In this case the decay vertex must be determined solely from the electron and positron tracks. The four photons are then assumed to have originated at the same point, and this assumption is used to calculate the overall invariant mass of the event. The $\pi^+\pi^-\pi^0$ mode has the advantage that the K_L decay vertex is known accurately from the charged pion tracks as well. Since all four tracks must originate at the same vertex, accidental backgrounds are negligible. Furthermore, Dalitz decay events, $K_L \to \pi^+\pi^-\pi^0(\pi^0 \to e^+e^-\gamma)$ are available which can be used to check the Monte Carlo calculation of the acceptance. Since the $\pi^0\pi^0\pi^0$ decays were collected using the E-731 neutral trigger, which required either four or six clusters in the lead glass calorimeter, Dalitz decay events in that mode (which would have had seven clusters) were rejected.

The main background to $\pi^0 \to e^+e^-$ in $K_L \to \pi^+\pi^-\pi^0$ decays in fact comes from π^0 Dalitz decays in which the photon is soft (less than 500 MeV), and is not detected or else overlaps with a shower produced by one of the other particles in the final state. Of couse, the e^+e^- invariant mass in a Dalitz decay must always be less than the π^0 mass; moreover, the matrix element for $\pi^0 \to e^+e^-\gamma$ falls rapidly with increasing M_{ee}, so the tail near the π^0 mass is very small. We estimate our current background level in this mode at about 2×10^{-8}.

Another potential background is the result of double Dalitz decays, $\pi^0 \to e^+e^-e^+e^-$, in which one e^+e^- pair is soft, so that both particles are swept out of the detector by the analysis magnet. As in the single-Dalitz case, the e^+e^- invariant mass must be less than the π^0 mass, however when all e^+e^- combinations are considered, the M_{ee} spectrum does not fall as quickly near the endpoint as it does in the single-Dalitz case. On the other hand, the double-Dalitz branching ratio is some 400 times smaller than that for single-Dalitz decays; in addition, we have found that we can efficiently reject these events by looking for the truncated upstream track segments left by the soft leptons.

One final background can contribute only to the $K_L \to \pi^0\pi^0\pi^0$ data. In this background process, two of the three π^0's undergo Dalitz decay. The two Dalitz photons accidentally combine to form a fake π^0, and an electron from one Dalitz decay and a positron from the other are lost at the magnet. This background is suppressed due to the requirement that two unrelated photons combine to form a fake π^0. However, it is dangerous in that the invariant mass of the observed e^+e^- pair need not be less than the π^0 mass; in fact, a roughly

flat M_{ee} distribution is expected from this background. As in the double-Dalitz case, cuts which reject events having evidence for extra upstream track segments are useful in reducing this background.

In addition the the Dalitz e^+e^- pairs, one must in the double-Dalitz and double-single-Dalitz cases include the effect of the approximately 0.6% of a radiation length of material in the trigger hodoscope and the first drift chamber. There is a probability of about 0.45% that a π^0 decay photon will convert in this material, leading to the production of another e^+e^- pair. This pair cannot by itself be mistaken for a $\pi^0 \to e^+e^-$ decay, since the measured e^+e^- invariant mass for such decays will always be less than about 20 MeV/c^2. It can, however, combine with a Dalitz pair (or with another pair from a second photon conversion) to generate backgrounds similar to those arising from double-Dalitz and double-single-Dalitz decays.

Combining all these backgrounds, we estimate the current background level to $\pi^0 \to e^+e^-$ from the $K_L \to \pi^0\pi^0\pi^0$ mode to be about 10^{-8} per K_L decay. The background is expected to come primarily from single Dalitz decays with photons overlapping other showers in the calorimeter. The background level is smaller than in the $K_L \to \pi^+\pi^-\pi^0$ case because it is possible to cut more tightly on the presence of extra energy in the calorimeter which may come from a soft photon. In the charged-mode case, such cuts must be looser, because when the charged pions shower in the lead glass, they often produce large, splotchy showers.

In the neutral-trigger data, we selected $\pi^0\pi^0e^+e^-$ candidate events by requiring:

- Two charged tracks with $p > 2.5$ GeV/c, oppositely charged, from a common vertex at least 138 meters, but no more than 158 meters, downstream of the target.
- Clusters in the lead glass calorimeter matched to both tracks, such that each track had $0.88 < E/p < 1.12$.
- Four additional, unmatched energy clusters in the lead glass. Defining Δz as the distance from the decay vertex determined from the charged tracks and the calorimeter, the squared invariant mass for the pair consisting of photons i and j is to a very good approximation given by

$$M_{ij}^2 = \frac{E_i E_j r_{ij}^2}{(\Delta z)^2},$$

where r_{ij} is the separation between cluster i and cluster j on the face of the calorimeter. We defined a χ^2 for the hypothesis that the four unmatched clusters were produced by the decay of two π^0's at the decay vertex as

$$\chi^2_{2\pi^0} = \min_{pairings}\left\{\frac{(M_{ij}-M_{\pi^0})^2}{\delta M_{ij}^2} + \frac{(M_{kl}-M_{\pi^0})^2}{\delta M_{kl}^2}\right\},$$

where the minimum is over the three possible pairings $(ij)(kl)$ of the four clusters and δM_{ij} is the estimated uncertainty in M_{ij}, primarily due to the lead glass energy resolution.

- The magnitude of the total transverse momentum of the six observed particles relative to the line of flight from the target to the decay vertex had to satisfy

$$(\sum \mathbf{p}_\perp)^2 < 300 \text{ MeV}^2/c^2,$$

in order to reduce backgrounds in which other decay particles were missed (for example, a photon from a π^0 Dalitz decay).

In the charged-trigger data, we wanted to identify $\pi^+\pi^-e^+e^-$ events. The requirements were:

- Four charged tracks, two positively and two negatively charged, originating at a common vertex at least 100 meters, but no more that 137 meters, downstream of the target, all with $p > 2.5$ GeV/c.
- Four clusters in the calorimeter, all with an energy greater than 500 MeV, each matched to one of the charged tracks; no clusters with energies greater than 1 GeV except for these four.
- E/p values less than 0.88 for one oppositely charged pair of tracks (the pion candidates) and between 0.88 and 1.12 for the other oppositely charged pair (the electron candidates).
- A total transverse momentum satisfying

$$(\sum \mathbf{p}_\perp)^2 < 300 \text{ MeV}^2/c^2,$$

again to reject K^0 decays with missing particles.

To reduce the number of background events from the single- and double-Dalitz decays processes (and from double photon conversions or photon conversions together with Dalitz decays), we imposed two additional cuts. First, in both the charged and neutral data, we looked for evidence of soft tracks which were bent out of the detector by the analysis magnet. We did this by considering all "extra" hits in the two drift chambers upstream of the magnet. We considered every pair consisting of one such hit in the first chamber and another in the second chamber. If the line connecting these two hits extrapolated to within 10 cm of the decay vertex determined from the fully reconstructed

tracks, then we threw out the event on the grounds that those hits might have been left by an additional, undetected track of the sort that might be present in Dailtz-decay or photon-conversion backgrounds. Monte Carlo simulations showed this cut to be quite effective at rejecting those backgrounds.

As an interesting check on the accuracy of the Monte Carlo simulation, we have looked in the charged-mode data for events representing the process $K_L \to \pi^+\pi^-\pi^0$ with a subsequent π^0 Dalitz decay, $\pi^0 \to e^+e^-\gamma$. We were able to reconstruct full some 6105 events consistent with being examples of that decay. Figure 11 shows the distribution of e^+e^- invariant masses for those events; also shown is the absolutely normalized prediction of the Monte Carlo. The distributions match very well above an e^+e^- mass of about 20 MeV/c^2. We attribute the excess in the data at low e^+e^- masses to $\pi^0 \to \gamma\gamma$ decays in which one of the photons converts in the approximately 0.006 radiation lengths of material between the decay volume and the first drift chamber.

In the neutral-mode data, we applied another cut designed to reduce the Dalitz decay background in which only a single soft photon is missed. This cut rejected any event in which an energy deposit of 120 MeV or more was observed in a single lead glass block which was *not* part of one of the identified clusters in the event. Because hadron showers are not necessarily well-contained in the three by three array of blocks forming a cluster, this cut could not be applied in the charged-mode analysis. In the neutral mode analysis, it effectively rejected the Dalitz decay background. To estimate the effect of this cut on the neutral-mode acceptance, we applied it to real $K_L \to \pi^0\pi^0\pi^0$ events in the data, whose kinematic characteristics are identical to those of $K_L \to \pi^0\pi^0\pi^0(\pi^0 \to e^+e^-)$ events, and determined what fraction of those events that would be have been rejected by the 120 MeV cut. As a result, we estimate that the acceptance for $\pi^0 \to e^+e^-$ in neutral mode is reduced by approximately 23% as a result of this cut.

In both samples, $\pi^0 \to e^+e^-$ decays will manifest themselves as events in which the e^+e^- invariant mass is close to the π^0 mass, and the total invariant mass is close to the K^0 mass. Based on Monte Carlo simulations, we defined a signal "box" in both final states, within which we look for $\pi^0 \to e^+e^-$ candidate events. In the neutral-mode analysis, the box extends 15 MeV/c^2 above and below the K^0 mass; in the charged-mode case, the resolution is better, so the box need extend only 10 MeV/c^2 to either side of the nominal K_L mass. In both cases, the e^+e^- mass had to be within 5 MeV/c^2 of the π^0 mass. This cut was fairly tight, in order to exclude as much as possible of the high-mass tail from the single-Dalitz decay backgrounds.

The scatter plots of M_{ee} versus $M_{\pi\pi ee}$ are shown in Figure 12. No events are observed in the box in either the charged- or the neutral-mode data.

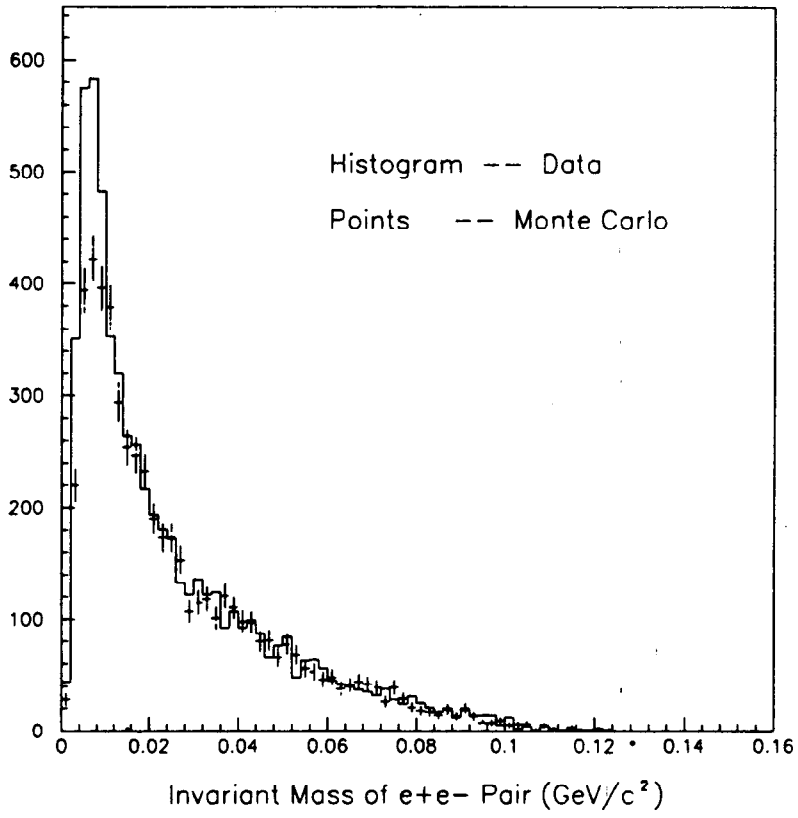

Figure 11: The distribution of e^+e^- invariant masses in events satisfying the criteria for $K_L \to \pi^+\pi^-\pi^0$ decays followed by a π^0 Dalitz decay, so that the fully reconstructed final state is $\pi^+\pi^-e^+e^-\gamma$. The solid histogram is the data; the points with error bars are from an absolutely normalized Monte Carlo simulation. The excess data at small masses are due to external photon conversions.

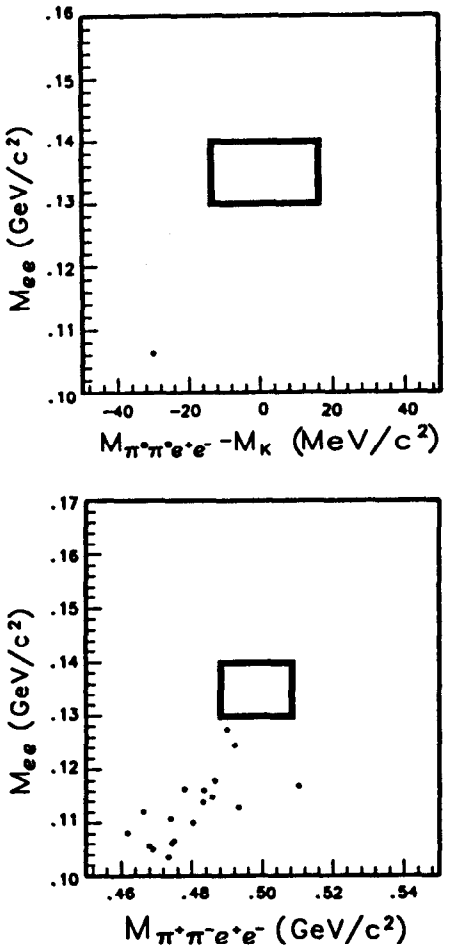

Figure 12: Scatter plots of e^+e^- invariant mass versus total invariant mass from the $\pi^0 \to e^+e^-$ search. The top plot shows the neutral-mode data; the bottom plot shows the charged-mode data. The boxes indicate the regions in which $\pi^0 \to e^+e^-$ signals would be expected, based on Monte Carlo simulations. No signal is observed.

To convert this non-observation into an upper limit on the branching ratio, we calculated our experimental acceptance for both trigger-modes using a Monte Carlo simulation. In the neutral-trigger mode, the average acceptance was 1.2%; in charged-trigger mode, the acceptance was double that. However, the total π^0 exposure from $K_L \to \pi^0\pi^0\pi^0$ was approximately 5.3×10^8 decays, compared to only 1.4×10^8 from $K_L \to \pi^+\pi^-\pi^0$. This difference was caused by three factors: most important is the fact that each $\pi^0\pi^0\pi^0$ decay gives three π^0 decays; also the branching ratio for $K_L \to \pi^0\pi^0\pi^0$ is nearly double that for $K_L \to \pi^+\pi^-\pi^0$. Finally, the intensity and running time for charged-trigger mode and neutral-trigger mode running were different.

Combining the acceptances and exposures, we have a single-event sensitivity for $\pi^0 \to e^+e^-$ of 1.57×10^{-7} in the $\pi^0\pi^0\pi^0$ mode, and 2.97×10^{-7} in the $\pi^+\pi^-\pi^0$ mode. The combined single-event sensitivity is therefore 1.02×10^{-7}. Since we see no events, we report a preliminary upper limit for the branching ratio $B(\pi^0 \to e^+e^-)$ of 2.3×10^{-7} at the 90% confidence level.

This result is consistent with the existing measurements and limits; however, it is only about half as stringent as the most recent upper limit of 1.3×10^{-7} from the SINDRUM experiment. Unlike the $\pi^- p$ scattering experiments, however, the technique described here is (so-far) background free. We estimate that the ultimate background level from the various processes discussed above is about $1\text{–}2 \times 10^{-8}$, with optimised cuts. Thus even at the unitarity limit of 4.8×10^{-8}, we expect a signal to noise ratio of two or better. To improve the current limit, or to see a signal, we basically need much greater exposure. This we expect to obtain in the summer of 1991, when a dedicated rare decay experiment, FNAL E-799, will run at Fermilab using the E-731 apparatus, with the addition of transition radiation detectors to improve π-e separation, a lead/scintillating fiber photon pre-converter to improve the resolution of nearby photons, and a new Level 2 charged trigger system. In that experiment, we anticipate observing a $\pi^0 \to e^+e^-$ signal of perhaps 20 events over a background of 10 or fewer.

REFERENCES

1) See, for example, G. Bélanger and C.Q. Geng, Phys. Rev. **D43,** 140 (1991), and references therein; see also J.M. Flynn and L. Randall, Nucl. Phys. **B326,** 31 (1989), (E) Nucl. Phys. **B334,** 580 (1990).

2) K.E. Ohl *et al.*, Phys. Rev. Lett. **64,** 2755 (1990).

3) A. Barker *et al.*, Phys. Rev. **D41,** 3546 (1990).

4) J.R. Patterson *et al.*, Phys. Rev. Lett. **64,** 1491 (1990).

5) L. Wolfenstein, Phys. Rev. Lett. **23,** 562 (1964).

6) G. Buchalla, A.J. Buras, and M.K. Harlander, Nucl. Phys. **B337,** 313 (1990).

7) H. Burkhardt *et al.*, Phys. Lett. **206B,** 169 (1988).

8) M. Karlsson *et al.*, Phys. Rev. Lett. **64,** 2976 (1990).

9) H. Galić, Phys. Rev. **D32,** 2456 (1985).

10) H. Taureg *et al.*, Physics Letters **65B,** 92 (1976).

11) A.S. Carroll *et al.*, Phys. Rev. Lett. **44,** 529 (1980).

12) Particle Data Group, Phys. Lett. **B239,** 1 (1990).

13) Y.C.R. Lin and German Valencia, Phys. Rev. **D37,** 143 (1988).

14) L. Rosselet *et al.*, Phys. Rev, **D15,** 574 (1977).

15) A.S. Carroll *et al.*, Phys. Lett. **96B,** 407 (1980).

16) A. Pais and S.B. Treiman, Phys. Rev. **168,** 1858 (1968).

17) P. Castoldi, J.-M. Frère, and G.L. Kane, Phys. Rev. **D39,** 2633 (1989).

18) N. Cabbibo and A. Maksymowicz, Phys. Rev. **137,** B438 (1965).

19) L. Bergström, Z. Phys. **C14,** 129 (1982).

20) Carsten Niebuhr *et al.*, Phys. Rev. **D40,** 2796 (1989).

21) A. Pich and J.Bernabéu, Z. Phys. **C22,** 197 (1984).

22) J. Fischer *et al.*, Phys. Lett. **73B,** 364 (1978).